consistent with their chemical oxidation as described above.

Reversible transfer of two electrons at the same potential has been reported recently for a number of inorganic and organometallic species.[45] However, particularly relevant to the work described herein is the study by Collman and co-workers of the $[Fe_2(CO)_6(PR_2)_2]^{2-/0}$ system,[40] where this phenomenon was rationalized in terms of the formation/cleavage of the Fe–Fe bond in the oxidized species. They also pointed out that simultaneous two-electron-redox behavior requires that the addition or removal of the second electron be more thermodynamically favorable than that for the first and hypothesized that structural rearrangement, i.e. metal–metal bond formation, allowed this energetic reversal in their system. Subsequently, Wojcicki[42] has reviewed the reactivity of several other dinuclear phosphido-bridged species with metal–metal bonding that undergo net two-electron behavior, although the lack of electrochemical data in many of the systems leaves some doubt as to whether the oxidation/reduction is truly simultaneous. Geiger[46] has reviewed and summarized the effect of structural changes (including metal–metal bond formation) on electrode reactions. Our recent studies[4-6] of the electrochemistry and chemistry of the Mo and W thiolate-bridged species $[M_2(CO)_8(SR)_2]^{2-/0}$ have confirmed the generality of simultaneous two-electron transfer for *dinuclear* complexes where metal–metal bonding is present in one form of the couple. The electrochemical data presented herein for the symmetric complexes $[M(SR)_4\{Mo(CO)_4\}_2]^{2-}$ are seemingly the first indication that this behavior can also occur in a *trinuclear* organometallic species, with the overall thermodynamics apparently governed by the formation of *two heterometallic* metal–metal bonds rather than one homometallic metal–metal bond. X-ray diffraction and/or EXAFS studies of these trinuclear complexes would substantiate this hypothesis.

Summary and Conclusions. The new trinuclear heterometallic carbonyl complexes $[M(SR)_4\{Mo(CO)_4\}_2]^{2-}$ (M = Fe, Co; R = Ph, Bz) have been prepared by a variety of related methods, including simply refluxing a mixture of $Mo(CO)_6$, an Fe salt, and $[NEt_4][SR]$ in MeCN. This formulation apparently has a high degree of thermodynamic stability and is likely to be produced in many systems involving synthesis of low-valent Fe–Mo–SR species. The complexes react with mono- and bidentate nucleophiles to form species resulting from attack at the central metal. The trinuclear species, formally containing a Mo(0)–Fe(II)–Mo(0) core, can be chemically oxidized by two electrons to the neutral $[M(SR)_4[Mo(CO)_4\}_2]$, which in turn can be formally classified as Mo(I)–Fe(II)–Mo(I). Electrochemical studies of this oxidation show that these two electrons are *removed at the same potential*, a rare phenomenon in heterometallic complexes that we attribute to a structural change induced by the formation of a pair of Fe–Mo bonds in the product.

Acknowledgment. We are indebted to Professor F. A. Schultz of Florida Atlantic University for many helpful discussions on the multielectron redox behavior of polynuclear systems. This work was supported by Grants 81-CRCR-1-0675 (to J.W.M. and W.E.N.) and 85-CRCR-1-1639 (to J.W.M.) from the USDA/SEA Competitive Grants Research Office.

(45) (a) Fenton, D. W.; Schroeder, R. R.; Lintvedt, R. L. *J. Am. Chem. Soc.* **1978**, *100*, 1931. (b) Fenton, D. E.; Lintvedt, R. L. *Ibid.* **1978**, *100*, 6367. (c) Lintvedt, R. L.; Kramer, L. S. *Inorg. Chem.* **1983**, *22*, 796. (d) Mandal, S. K.; Nag, K. *Ibid.* **1983**, *22*, 2567. (e) Louis, R.; Angus, Y.; Weiss, R.; Gisselbrecht, J. P.; Gross, M. *Nouv. J. Chim.* **1981**, *5*, 71. (f) Hollis, L. S.; Lippard, S. J. *J. Am. Chem. Soc.* **1981**, *103*, 6761. (g) Hollis, L. S.; Lippard, S. J. *Inorg. Chem.* **1983**, *22*, 2605. (h) Moraczewski, J.; Geiger, W. E., Jr. *J. Am. Chem. Soc.* **1978**, *100*, 7429. (i) Finke, R. G.; Voegeli, R. H.; Laganis, E. D.; Boekelheide, V. *Organometallics* **1983**, *2*, 347.

(46) Geiger, W. E. *Prog. Inorg. Chem.* **1985**, *33*, 275.

(47) The periodic group notation in parentheses is in accord with recent actions by IUPAC and ACS nomenclature committees. A and B notation is eliminated because of wide confusion. Groups IA and IIA become groups 1 and 2. The d-transition elements comprise groups 3 through 12, and the p-block elements comprise groups 13 and 18. (Note that the former Raman number designation is preserved in the last digit of the new numbering: e.g., III → 3 and 13.)

Contribution from the Kenan Laboratories of Chemistry, The University of North Carolina, Chapel Hill, North Carolina 27514

Electron Diffusion in Wet and Dry Prussian Blue Films on Interdigitated Array Electrodes

B. J. Feldman and Royce W. Murray*

Received September 2, 1986

The rate of electron transport has been measured in films of ferric ferrocyanide (Prussian blue, Fe(III/II)) coated on interdigitated array electrodes. By control of the electrode potentials, the films can be (1) partially reduced to the Fe(III/II)–Fe(II/II) mixed-valent state, (2) partially oxidized to the Fe(III/II)–Fe(III/III) mixed-valent state, and (3) disproportionated in the absence of solvent to contain both mixed-valent states, arranged spatially in series between the electrodes. Results show that the rate of electron transport, measured as the electron diffusion coefficient, D_e, in Fe(III/II)–Fe(II/II) mixed-valent films is surprisingly insensitive to which alkali-metal counterion is employed in the contacting electrolyte solution. The microscopic (local) lattice mobility of the counterion must exceed the electron mobility associated with self-exchange between Fe(III/II) and Fe(II/II) sites. In KNO_3 electrolyte, it is also shown that there are two electrochemically distinct Fe(III/II)–Fe(II/II) couples, which differ by about a factor of 10 in their electron-transport rates. The electron diffusion rate in Fe(III/II)–Fe(III/III) mixed-valent films yields an estimate for the electron self-exchange rate constant for ferricyanide and ferrocyanide lattice sites in Prussian blue, 1.3×10^6 M^{-1} s^{-1}, that is about 10 times larger than any known k_{ex} rate constant for the analogous homogeneous solution reaction. When exposed only to a bathing gas, Prussian blue films exhibit steady-state, solid-state voltammograms at potentials that can drive disproportionation of the Fe(III/II) material by oxidizing and reducing it at opposing electrode/film interfaces. The solid-state currents are critically dependent on the presence of water vapor in the bathing gas and vanish in dry N_2. Removal of the interstitial water in Prussian blue apparently lowers the local counterion mobility so severely as to become limiting upon the electron mobility.

The observation[1a] of electrochemical reactivity of thin-film coatings of the mixed-valent compound ferric ferrocyanide (Prussian blue) on electrodes has sparked a number of recent investigations.[1-4] Appealing features of these films include their

0020-1669/87/1326-1702$01.50/0

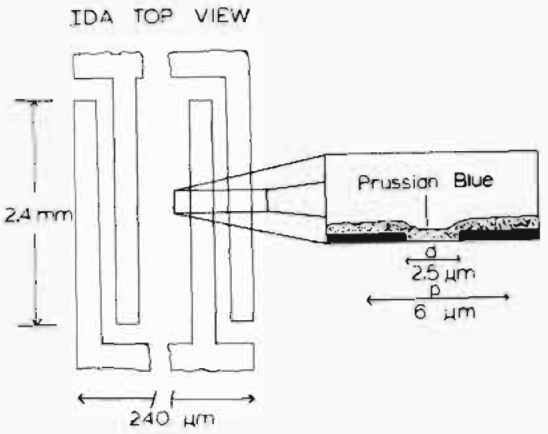

Figure 1. Schematic diagram of the IDA electrode. Inset shows one finger pair coated with electrodeposited Prussian blue.

facile preparation, their potential for electrocatalytic,[2d] electrochromic,[2f] and charge storage[1d] applications, and their extension to related mixed-metal cyanide films.[5,6] There is however, relatively little known[1c,2g,7] about the dc electron conductivity of Prussian blue films. In a solvated Prussian blue lattice containing a gradient of reduced and oxidized Fe sites and appropriate charge compensating counterions, it can be expected that electron transport would occur by electron hopping (electron self-exchange) between neighboring oxidized and reduced Fe sites. This is also called "redox conduction"[8] and is characterized by the "electron diffusion coefficient", D_e.

We were attracted to Prussian blue because it presented an opportunity to study multiple-electron-transport pathways, and their environmental dependance, in a material more internally ordered than most polymeric, electroactive materials.[9] Electrochemically deposited, blue films of Prussian blue[1a,2a,b,7b] contain two kinds of iron, high-spin iron Fe(III) states and ferrocyanide as low-spin Fe(II), abbreviated here as Fe(III/II). Thin Prussian blue films on electrodes can be oxidized and reduced in two widely separated, well-defined cyclic voltammetric waves in aqueous[1-3] and organic[4b] solvents that correspond to the reactions Fe(III/II) → Fe(III/III), green to golden, and Fe(III/II) → Fe(II/II), white, respectively. The Fe(III/II)–Fe(III/III) and Fe(III/II)–Fe(II/II) mixed-valent compositions that exist in the lattice compound during these reactions offer the possibility of electron transport by two different mechanisms, i.e., electron hopping between neighboring oxidized and reduced low-spin Fe sites and electron hopping between neighboring oxidized and reduced high-spin Fe sites, respectively.

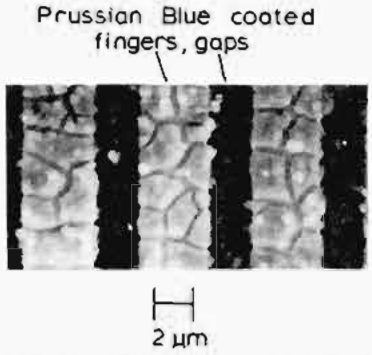

Figure 2. SEM micrograph of the Prussian blue coated IDA: magnification, 5610; accelerating voltage, 15 kV; Prussian blue thickness, 0.68 μm.

This paper describes the electron conductivity of Prussian blue films in three different settings: (i) films in the Fe(III/II)–Fe(II/II) mixed-valent state and in contact with aqueous electrolytes containing different alkali-metal cations; (ii) films in the Fe(III/II)–Fe(III/III) mixed-valent state in contact with aqueous KNO_3 electrolyte; (iii) films containing regions of Fe(III/II)–Fe(II/II) *and* Fe(III/II)–Fe(III/III) mixed-valent states, arranged spatially in series, and contacted only by a gaseous environment (*solid-state voltammetry*). Thus, for a single, well-ordered material, we describe the effects of countercation size, lattice oxidation state, and solvent population upon electron conductivity. A picture of the circumstances under which ionic motions within the Prussian blue lattice can or cannot influence electron conductivity emerges from the experimental results.

Microlithographically defined interdigitated array (IDA)[10] electrodes were coated with Prussian blue films for the electron-conductivity studies. The use of microarray electrodes for the study of electroactive films has been pioneered by Wrighton and co-workers.[11] Our IDA consists of multiple pairs of 3.5-μm-wide Pt finger electrodes separated by 2.5-μm gaps of borosilicate glass substrate, both fingers and gaps being coated with Prussian blue as schematically illustrated in Figure 1. The IDA gives steady-state electron-conduction currents; this was desirable in the present study for the following reason. In an experiment to measure D_e for the Fe(III/II)–Fe(II/II) mixed-valent state in contact with aqueous KNO_3, for example, the two IDA electrode potentials are set so as to drive the Fe(III/II) → Fe(II/II) reduction at one film/electrode interface and the Fe(II/II) → (Fe(III/II) oxidation at the other. Steady-state concentration gradients of the two high-spin Fe oxidation states (e.g., an electron-free energy gradient[12]) and of K^+ counterions that have entered from the contacting solution and a steady-state current flow are developed across the film. In the *steady state*, there is *no macroscopic counterion flow*, and any effects of motions of the lattice counterions on D_e will be only the fundamentally more interesting *local* ones, i.e., those associated with the micoscopic event of an electron hopping from a Fe(II/II) site in the Prussian blue lattice to a Fe(III/II) site.

Experimental Section

All reagents were used as received. Fabrication and mounting of IDA electrodes has been described previously.[10a] Electrochemistry was performed with a Pine Instruments Model ARDE 3 bipotentiostat in an N_2-degassed cell with glass-frit-separated compartments for NaSCE

(1) (a) Neff, V. D. *J. Electrochem. Soc.* **1978**, *125*, 886. (b) Ellis, D.; Eckhoff, M.; Neff, V. D. *J. Phys. Chem.* **1981**, *85*, 1225. (c) Rajan, K. P.; Neff, V. D. *J. Phys. Chem.* **1982**, *86*, 4361. (d) Neff, V. D. *J. Electrochem. Soc.* **1985**, *131*, 1382.
(2) (a) Itaya, K.; Akahoshi, H.; Toshima, S. *J. Electrochem. Soc.* **1982**, *129*, 1498. (b) Itaya, K.; Ataka, T.; Toshima, S. *J. Am. Chem. Soc.* **1982**, *104*, 4767. (c) Itaya, K.; Ataka, T.; Toshima, S.; Shinohara, T. *J. Phys. Chem.* **1982**, *86*, 2415. (d) Itaya, K.; Uchida, I.; Toshima, S. *J. Phys. Chem.* **1983**, *87*, 105. (e) Itaya, K.; Uchida, I.; Toshima, S.; De La Rue, R. M. *J. Electrochem. Soc.* **1984**, *131*, 2086. (f) Itaya, K.; Shibayama, K.; Akahoshi, H.; Toshima, S. *J. Appl. Phys.* **1982**, *53*, 804. (g) Itaya, K.; Uchida, I.; Neff, V. D. *Acc. Chem. Res.* **1986**, *19*, 162.
(3) (a) Mortimer, R. J.; Rosseinsky, D. R. *J. Electroanal. Chem. Interfacial Electrochem.* **1983**, *151*, 133. (b) Mortimer, R. J., Rosseinsky, D. R.; *J. Chem. Soc., Dalton Trans.* **19844**, 2059.
(4) Crumbliss, A. L.; Lugg, P. S.; Patel, D. L.; Morosoff, N. *Inorg. Chem.* **1983**, *22*, 3541. (b) Crumbliss, A. L.; Lugg, P. S.; Morosoff, N. *Inorg. Chem.* **1984**, *23*, 4701.
(5) (a) Sinha, S.; Humphrey, B. D.; Fu, E.; Bocarsly, A. B. *J. Electroanal. Chem. Interfacial Electrochem.* **1984**, *162*, 351. (b) Sinha, S.; Humphrey, B. D.; Bocarsly, A. B. *Inorg. Chem.* **1984**, *23*, 203. (c) Rubin, H.; Humphrey, B. D.; Bocarsly, A. B. *Nature (London)* **1984**, *308*, 5957.
(6) Siperko, L. M.; Kuwana, T. *J. Electrochem. Soc.* **1983**, *130*, 396.
(7) (a) Viehback, A.; DeBerry, D. E. *J. Electrochem. Soc.* **1985**, *132*, 1369. (b) Itaya, K.; Uchida, I.; Neff, V. D. *Acc. Chem. Res.* **1986**, *19*, 162.
(8) Pickup, P. G.; Kutner, W.; Leidner, C. R.; Murray, R. W. *J. Am. Chem. Soc.* **1984**, *106*, 1991.
(9) Murray, R. W. *Annu. Rev. Mater. Sci.* **1984**, *14*, 145.
(10) (a) Chidsey, C. E. D.; Feldman, B. J.; Lundgren, C.; Murray, R. W. *Anal. Chem.* **1986**, *58*, 145. (b) Feldman, B. J.; Murray, R. W. *Anal. Chem.* **1986**, *58*, 2844.
(11) (a) White, H. S.; Kittlesen, G. P.; Wrighton, M. S. *J. Am. Chem. Soc.* **1984**, *106*, 5375. (b) Kittlesen, G. P.; White, H. S.; Wrighton, M. S. *J. Am. Chem. Soc.* **1984**, *106*, 7389. (c) Paul, E. W.; Ricco, A. J.; Wrighton, M. S. *J. Phys. Chem.* **1985**, *89*, 1441. (d) Thackeray, J. W.; White, H. S.; Wrighton, M. S. *J. Phys. Chem.* **1985**, *89*, 5133. (e) Kittlesen, G. P.; White, H. S.; Wrighton, M. S. *J. Am. Chem. Soc.* **1985**, *107*, 5375. (f) Wrighton, M. S. *Comments Inorg. Chem.* **1985**, *4*, 269.
(12) Chidsey, C. E. D.; Murray, R. W. *J. Phys. Chem.* **1986**, *90*, 1479.

reference, IDA, and Pt auxiliary electrodes. Before Prussian blue deposition, the IDAs were reductively galvanostated in 1 M HCl at 50 μA (ca. 10 mA/cm^2) for 1 min. Prussian blue deposition was with both fingers of the IDA held at constant potential (0.5 V vs. NaSCE) in a solution 2 mM in $FeCl_3$ (Merck) and in $K_3Fe(CN)_6$ (Allied Chemical), 10 mM in HCl, and 20 mM in KCl. The microcomputer-monitored deposition was terminated when a suitable charge (typically 20 mC/cm^2) had been passed. A typical film is 0.1–1 μm thick and may contain the equivalent of 5–50 mC/cm^2 of Fe sites. The Prussian blue coated IDAs were either used immediately or stored in a water-saturated atmosphere to prevent cracking[2b] of the Prussian blue film caused by rapid drying. The importance, for electron conductivity measurements, of avoiding drying is illustrated in the SEM of a very thick film in Figure 2 where drying (necessarily) and apparent lateral shrinkage of the film has occurred.

Formulas that have been suggested for Prussian blue include $Fe_4[Fe(CN)_6]_3$ (so-called "insoluble" Prussian blue) and $C^+Fe(Fe(CN)_6]$ (so-called "soluble" Prussian blue), where C^+ is a monovalent cation. The "insoluble" form of Prussian blue is also known to contain a considerable amount of both coordinated and interstitial water.[13] While controversy exists[2g] as to the actual composition of electrochemically grown films, our own energy-dispersive X-ray analysis studies[14] show that as-grown films contain little or no C^+, and cannot be the "soluble" form. On the other hand, films that have been electrochemically reduced and then reoxidized in, for example, aqueous KNO_3 or CsCl, have incorporated some electrolyte cation, showing atom ratios K/Fe = 0.14 and Cs/Fe = 0.14 (by EDX). The expected values are 0.5 and zero for the "soluble" and "insoluble" forms, respectively, suggesting that electrochemically cycled films are actually a mixture of the two stoichiometries (ca. one-third "soluble" form). Except for specified solid-state voltammetry experiments, all films on the IDAs used for electron-conductivity studies in contact with aqueous electrolyte have been previously cycled in that particular electrolyte (to determine Q, vide infra), and are thus mostly, but not entirely, "insoluble" Prussian blue.

Profilometry of the films was performed on a Tencor Alpha-step 100 profiler with a 12.5-μm-diameter stylus at a scan rate of 0.01 mm/s. Optical microscopy was performed with a Zeiss Universal microscope. Scanning electron micrographs were obtained with an ICI Model DS-130.

Measurement of D_e for Films Contacted by Aqueous Electrolyte Solutions. D_e was measured by two schemes, each consisting of a pair of experiments that determine the accessible electroactive charge (Q) of and the steady-state electron-conduction current i_{lim} across the Prussian blue film.

The first scheme, which we term *steady-state voltammetry*, involves, first, shorting the two Pt finger sets of a coated IDA together to form a common working electrode and cyclically sweeping their potential (relative to a NaCl-saturated SCE reference electrode) over the interval +0.5 to −0.2 V vs. NaSCE at a scan rate (5 mV/s) slow enough for all of the Prussian blue in the IDA gap to react. The total charge (Q) measured under the second (and thereafter reproducible) of the resulting Fe(III/II) → Fe(II/II) cyclic voltammograms gives the quantity of electroactive high-spin Fe in the film. Next, the potentials of the two Pt finger sets are controlled independently, with one IDA scanned at 5 mV/s through either the Prussian blue reduction (i.e., to −0.2 V, to measure D_e for Fe(III/II) → Fe(II/II) reduction) or oxidation (i.e., to 1.1 V, to measure D_e for Fe(III/II) → Fe(III/III) oxidation). The ratio of the steady-state current i_{lim}, taken from the resulting voltammetric plateau, to the charge Q gives D_e (vide infra).

The second scheme for D_e is similar, but is more sensitive to whether D_e varies for different mixed-valent Fe(III/II)–Fe(II/II) compositions in the film in between the extremes of Fe(III/II) and Fe(II/II). This scheme involves a pair of experiments labeled *staircase coulometry* and *scanning conductivity*. Staircase coulometry[15] resembles cyclic voltammetry of the Prussian blue coated IDA except that the IDA fingers are shorted together and their potential is advanced (relative to NaSCE) through the voltammetric wave in 20-mV (step) increments. The charge Q_{sc} passed to bring the film into equilibrium with the new electrode potential is measured for each increment, by extrapolating the linear portion of the 120 s long charge/time plot to zero time. In scanning conductivity, the IDA potential is again advanced incrementally in 20-mV steps but with a 20-mV potential difference between the two Pt IDA finger sets. The steady-state current i_{ss} flowing between the Pt finger sets is measured after a 120-s equilibration period. The ratio of i_{ss} and Q_{sc} measured after each potential increment leads to D_e for that potential interval.

Solid-State Voltammetry. In solid-state experiments, there is no solvent or reference electrode; the Prussian blue coated IDA (typical film thicknesses were 0.25–1 μm) is simply exposed to the chosen gas and a potential difference applied across the two IDA electrode terminals is slowly scanned to a value sufficient to oxidize Fe(III/II) at one terminal and reduce it at the other (i.e., to disproportionate the Fe(III/II) in the IDA gap). D_e values are not measured in this experiment. Film preparation was as described above. The bathing gases were dry (tank) N_2, moist N_2 (bubbled through distilled H_2O), or moist room air.

Results

Redox conductivity or electron transport through a Prussian blue film via electron hopping or self-exchange between, for example, neighboring Fe(III/II) and Fe(II/II) sites is described by Fick's first law. Electron motion is driven by concentration gradients of Fe(III/II) and Fe(II/II) sites in the Prussian blue film in the IDA gap (see Figure 1), and the electron mobility, given as an electron diffusion coefficient, D_e, is[10a]

$$D_e = (i_{lim}/Q)(dpN)/(N-1) \quad (1)$$

where i_{lim} is the limiting steady-state current obtained when the Pt finger potentials are set to completely reduce (i.e., to Fe(II/II)) and oxidize (i.e., to Fe(III/II)) opposite sides of the film, N is the number of fingers (41 in our array, 20 and 21 extending from opposing contact pads), Q is the total charge for converting the film between the Fe(III/II) and Fe(II/II) forms, d and p are dimensions as in Figure 1, and diffusion–migration terms[16] are neglected. This remarkably simple equation does not contain the electroactive site concentration or film thickness, which are often difficult to specify without assumptions, but does require that the Prussian blue coating be uniformly thick on both Pt fingers and in the gap and that the thickness of the deposited film be less than (or not much greater than) the Pt finger height (0.3 μm in our IDA). We have satisfactorily established[10b] these points by a combination of surface profilometry and SEM micrographs. In a situation where the profilometer stylus could interrogate both finger tops and the gaps, we established both that the Prussian blue films were of equal thickness on finger tops and in the gaps and that the determined film density agreed with a published value.[13a] Also, we have shown[10b] that D_e from eq 1 is independent of Prussian blue film thickness for films between 0.25 and 1.0 μm thick. These results establish the validity of eq 1 for the present study.

Steady-State Voltammetry. D_e for the Fe(III/II)–Fe(II/II) Mixed-Valent State in Contact with Various Electrolytes. Experiments to determine how fast electrons diffuse by hopping between Fe(III/II) and Fe(II/II) high-spin Fe sites in Fe(III/II)–Fe(II/II) mixed-valent films are illustrated in Figure 3 for films in contact with KNO_3 and RbCl electrolytes.

Considering the KNO_3 electrolyte, Figure 3A is a cyclic voltammogram obtained by shorting the Pt fingers together and scanning their potential through the Fe(III/II) → Fe(II/II) reduction wave. The resulting voltammogram has a somewhat pointy central peak centered at $E^{\circ\prime}$ = 0.19 V. Although difficult to discern from Figure 3A, published voltammograms[1a,2b] show, and we have verified,[10a] that this central peak usually has shallow shoulders on the negative and sometimes the positive sides. The overall charge Q under the voltammetric peak represents the amount of electroactive high-spin Fe. Parts B and C of Figure 3 represent[17] currents at the two Pt IDA fingers when the potential of one finger (Figure 3B) is scanned negatively to produce Fe(II/II), while that of the other (Figure 3C) is maintained at 0.5 V, generating Fe(III/II) there, causing a steady-state flow of electrons down the concentration gradients of Fe(II/II) and Fe(III/II) sites in the interelectrode gap. The limiting currents i_{lim} of the voltammograms at the two Pt fingers (Figure 3B,C)

(13) (a) Ludi, A.; Gudel, H. V. *Struct. Bonding (Berlin)* **1973**, *14*, 1. (b) Buser, H. J.; Schwarzenback, D.; Petter, W. A. *Inorg. Chem.* **1977**, *16*, 2704.
(14) Lundgren, C.; Murray, R. W., unpublished results, 1985.
(15) Su, C.; Heineman, W. R. *Anal. Chem.* **1981**, *53*, 594.
(16) Buck, R. P., private communication, 1985.
(17) Curves B and C differ because of the need, on the Pt finger whose potential is being scanned (Curve B), to reduce the film resting atop it, and to inject a net reduction charge into the film in the gap to generate the Fe(II/II) gradient there.

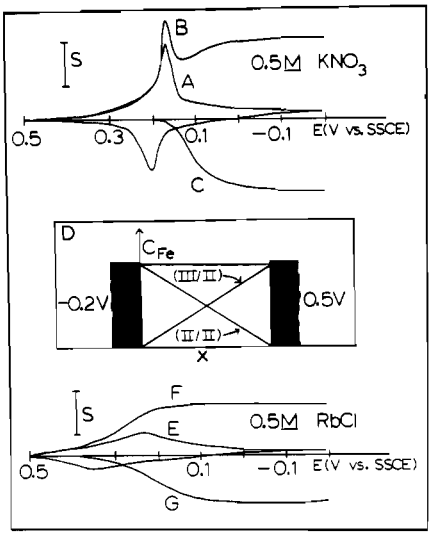

Figure 3. Steady-state reductive voltammetry at a Prussian blue coated IDA [(A, B, C) 0.5 M KNO_3, pH 4; (E, F, G) 0.5 M RbCl, pH 4]: (A, E) cyclic voltammetry with the potentials of both Prussian blue coated IDA terminals scanned simultaneously; (B, F) currents resulting from scanning one terminal while the opposite terminal (C, G) is maintained at 0.5 V; (D) Fe concentration–distance profiles in the IDA gap at potentials of plateau regions in curves B, C, F, and G. v = 5 mV/s. S = 1 μA (A, E), 0.5 μA (B, C, F, G). Prussian blue thickness is 0.45 μm.

are equal in magnitude and oppositely signed; at i_{lim} the Fe(III/II) and Fe(II/II) gradients are completely polarized as illustrated in Figure 3D. The result[18] for D_e in KNO_3, calculated with thus determined Q and i_{lim} from eq 1, is given in Table I, as are the cyclic voltammetric $E^{\circ\prime}$ and half-wave potential $E_{1/2}$ taken from Figure 3C.

Analogous experiments in other electrolytes (e.g., RbCl in Figure 3E–G) are qualitatively similar, except that the voltammetry shows that the time required for cations to migrate into the film to charge the film to a steady-state condition is much slower in Cs^+ and Na^+ electrolyte than in K^+, NH_4^+, or Rb^+ electrolyte. Results for D_e, $E^{\circ\prime}$, and $E_{1/2}$ are collected in Table I. The $E^{\circ\prime}$ values for films deposited on IDAs range from 0.406 V for Cs^+ to 0.082 V for Na^+. The variation in $E^{\circ\prime}$ that we observe is a regular progression and reflects a cation-dependent stabilization of the Fe(II/II) oxidation state similar to that observed for other metal cyanide complexes.[5] The most important point in Table I, however, is that values of $E^{\circ\prime}$ and $E_{1/2}$ differ; we will return to this later.

With the possible exception of a slowed electron diffusion in $NaNO_3$ electrolyte, the results in Table I show that the electron diffusion rate D_e in Fe(III/II)–Fe(II/II) mixed-valent films is remarkably insensitive to the cation that enters the lattice as a counterion to the Fe(II/II) state. This is in marked and surprising contrast to the substantial differences in oxidation-state stabilization by different cations evidenced in the strong variation of $E^{\circ\prime}$ and to the qualitatively different *net* film charging rates in the presence of the different cations. It is important at this point to remember that the D_e experiment, as we have conducted it, depends on electrons hopping between Fe(III/II) and Fe(II/II) sites in a film that has achieved a *macroscopic steady-state*,

Table I. Electron Diffusion Coefficients of D_e and Potentials for Prussian Blue Fe(III/II)–Fe(II/II) Mixed-Valent Films with Various Electrolytes

electrolyte[a]	$E^{\circ\prime}$,[b] V vs. NaSCE	$E_{1/2}$,[c] V vs. NaSCE	$10^9 D_e$, cm^2/s	no. of expts
0.5 M $NaNO_3$	0.082[d]	0.049	0.80	1
0.5 M KNO_3	0.19[e]	0.14	3.9 ± 1.3[f]	8
0.5 M NH_4Cl	0.225[g]	0.168	8.2 ± 2.8	2
0.5 M RbCl, $RbNO_3$	0.297[h]	0.261	6.6 ± 2.0	4
0.5 M CsCl	0.406[i]	0.328	3.3	1
0.5 M KNO_3[j]	0.19	0.14	(0.3 ± 0.04)[j]	3

[a] All electrolyte solutions adjusted to pH 4. [b] Formal potential is average of reduction and oxidation E_{peak} in cyclic voltammetry at 5 mV/s. [c] Potentials at $^1/_2 i_{lim}$ for steady-state voltammograms like parts C and G of Figure 3, at 5 mV/s; average of negative and positive scans. [d] Other values are 0.08[14] and 0.03 V[4b] (converted from Ag/AgCl reference). Like that in ref 4b, our voltammetry in aqueous $NaNO_3$ is well-defined and quite stable, in contrast to that described by Itaya et al.,[2b] which for their galvanostatically prepared films was unstable. [e] Other values are 0.195,[1b] 0.19,[2b] 0.18,[4b] (converted from Ag/AgCl reference), and 0.187 V.[14] [f] Previous chronoamperometric determination gave (2.7–5) × 10^{-9} cm^2/s. [g] Other values are 0.18[2b] (estimated from Figure 6) and 0.22 V.[14] [h] Other values are 0.31[2b] (estimated from Figure 6) and 0.34 V.[14] [i] Other values are 0.10[2b] and 0.46 V[2b] (estimated from Figure 6) and 0.41 V.[14] We do not observe the voltammetric feature at 0.10 V reported in ref 2b. [j] Conducted on Prussian blue coated IDAs that had been allowed to dry.

constant concentration of these sites and of the counterion present. The *local* counterion motion that accompanies an electron-hopping event is in this circumstance probably quite small and comparable to dimensions dictated by the Prussian blue lattice as illustrated in

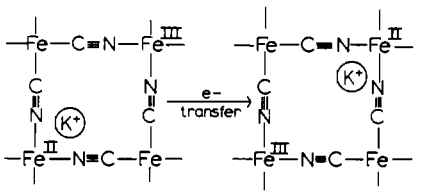

The importance of *local* counterion motions in solid-state electron-transfer dynamics in dialkylbiferrocenium salts was recently pointed out by Hendrickson et al.[20] In the present case, Na^+ excepted, the insensitivity of D_e to the cation identity implies that the *local* cation motions can occur so rapidly as to not control the rate of electron-hopping reaction. Just as Hendrickson et al. found[21] with a different solid-state example, however, we will show below, using solid-state voltammetry, that lattice solvation can have a profound effect on electron-hopping rates.

Dependence of D_e on Fe(III/II)–Fe(II/II) Mixed-Valent-State Composition (Electrode Potential). The $E_{1/2}$ of the IDA redox conduction wave in Figure 3C represents the formal potential of the redox couple by which the electron diffusion occurs and, in the simplest of situations, should equal the cyclic voltammetric formal potential $E^{\circ\prime}$ measured from the average of the reduction and oxidation E_{peak} values. Table I shows, however, that in each supporting electrolyte, $E_{1/2}$ is 33–78 mV more negative than the cyclic voltammetric $E^{\circ\prime}$. This result raised the possibility that D_e is not potential-independent, but varies according to the different mixtures of Fe(III/II) and Fe(II/II) states formed between the limits of a totally Fe(III/II) and a totally Fe(II/II) film.

This phenomenon was further investigated in 0.5 M KNO_3 electrolyte by using staircase coulometry and scanning conductivity (see Experimental Section), in which charge Q_{sc}, and electron conduction current, i_{ss}, are evaluated for small (20 mV) variations of the two Pt finger potentials (and small variations in the average Prussian blue oxidation state). In staircase coulometry, we measure the charge Q_{sc} passed to bring the oxidation state of a

(18) These results are for films kept in a moist atmosphere and never dried between film deposition and study of D_e. While films that had been allowed to dry exhibited quite similar cyclic voltammograms (indicating that most of the deposit was still electrochemically accessible to at least one Pt finger), the dried films gave depressed D_e values (see parenthetical result in Table I). SEM (Figure 2) shows clearly that drying leads to cracking of the film; it is likely these cracks present interruptions in the electron diffusion pathway between the fingers. Cracking of Prussian blue films upon drying has been recognized.[2b]

(19) These values agree quite well for all the cations with $E^{\circ\prime}$ values determined in this laboratory[14] for Prussian blue films potentiostatically deposited on conventional Pt-disk electrodes, and for K^+, NH_4^+, and Rb^+ with others' results.[2b,4b] They do not agree[2b,4b] for Na^+ and Cs^+. (See Table I, footnote, for the details.)

(20) Rheingold, A. L.; Sano, H.; Motoyama, I.; Nakashima, S. *J. Am. Chem. Soc.* **1985**, *107*, 7996.

(21) Oh, S. M.; Hendrickson, D. N.; Hassett, K. L.; Davis, R. E. *J. Am. Chem. Soc.* **1985**, *107*, 8009.

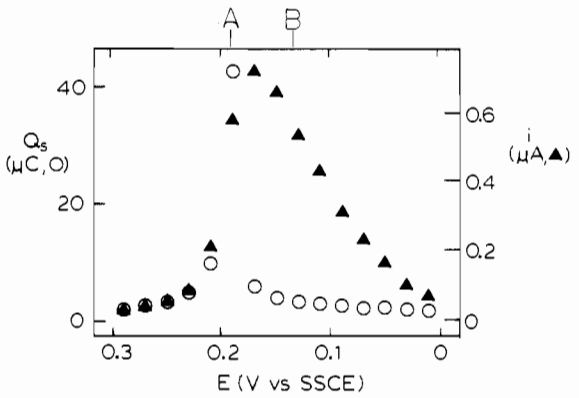

Figure 4. Staircase coulometry (Q_{sc}, ○) and scanning conductivity (i_{ss}, ▲) from a Prussian blue coated IDA in 0.5 M KNO_3, pH 4. For staircase coulometry, potential step = 20 mV and integration time = 120 s. For scanning conductivity, ΔE = 20 mV and equilibration time = 120 s. Prussian blue thickness = 1.06 μm. See text for the definition of A and B.

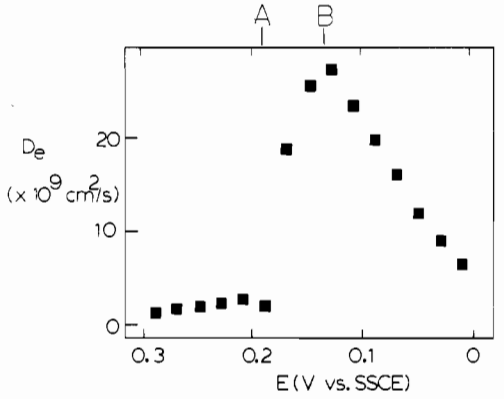

Figure 5. Electron diffusion coefficient (D_e) for high-spin Fe as a function of electrochemical potential. See text for the definition of A and B.

Prussian blue film into equilibrium with the applied potential when that potential is changed in 20 mV increments (Figure 4(○)). The same IDA specimen is then evaluated by the scanning conductivity experiment, in which the potentials of the two IDA finger pairs differ by 20 mV and the potential of each is advanced in 20-mV increments and allowed to equilibrate. This results in a steady-state current, i_{ss} (Figure 4(▲)), due to shallow Fe(II/II)/Fe(III/II) concentration gradients established across the gap after each incremental change in potential. Clearly, the normalized Q_{sc} and i_{ss} results in Figure 4 are not superimposable as would be the case for a single, homogeneous redox couple in the limit of noninteracting electrons and constant counterion activity.[12]

At each electrode potential in Figure 4, the Q_{sc} and i_{ss} values are proportional, respectively, to the redox capacity (ρ, F/cm^3) and the (electron free energy gradient-driven) electron conductivity (σ_e, Ω^{-1} cm^{-1}) of the Prussian blue film. We have shown[12] that D_e equals the ratio of ρ and σ_e, and it follows that

$$D_e = \sigma_e/\rho = (i_{ss}/Q_{sc})(dpN)/(N - 1) \qquad (2)$$

D_e values thus derived from Figure 4 are shown in Figure 5 and confirm that the electron-hopping rates vary substantially as the overall ratio of Fe(III/II) and Fe(II/II) oxidation states in the film changes with the electrode potential.

The most plausible explanation of Figure 5 is in reference to the presence of the more negative shoulder, at ca. 0.14 V, on the main cyclic voltammetric peak of Figure 3A that we referred to earlier. The presence of *two voltammetrically distinct high-spin Fe states* could offer two pathways for electron conduction. In Figure 5, for all the Fe sites that are electroactive at potentials from ca. 0.3 V to ca. 0.19 V, D_e is relatively constant at (2–3) × 10^{-9} cm^2/s. This potential interval includes approximately 73% of the reducible sites and the major peak of the cyclic voltammogram from which the $E^{\circ\prime}$ of 0.19 V (potential "A" in Figure 5) was estimated. For the sites that are reduced at more negative potentials, D_e rapidly increases by over 10-fold, reaches a maximum at ca. 0.13 V, and then gradually decreases.[22] This latter, more conductive, potential interval includes the formal potential 0.14 V estimated for the negative shoulder on the cyclic voltammogram (potential "B" in Figure 5), and ca. 27% of the reducible Fe. In other words, there seem to be two different Fe species, the *less prevalent one exhibiting a substantially faster electron self-exchange rate.*

We believe the following is a reasonable hypothesis concerning the chemical nature of the two differently conducting Fe sites. Single-crystal X-ray studies of the "insoluble" form of Prussian blue,[13] $Fe_4[Fe(CN)_6]_3$, suggest a structure in which there are two types of high-spin Fe, one coordinated to four isocyano ligands and two water molecules (labeled type "A"), and one in which the Fe is hexacoordinated with isocyano ligands (labeled type "B"):

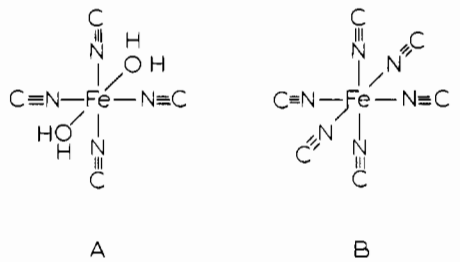

Type "A" has an occupancy of 75% and type "B" 25%. Although our Prussian blue films undoubtedly have considerable disorder, as described in the Experimental Section, our compositional studies come closer to the "insoluble" stoichiometry than to the so-called "soluble" form. The formal potential for the type "A" Fe should be the more positive of the two, as reasoned by analogy with $Fe(H_2O)_6^{3+}$ ($E^{\circ\prime}$ = 0.54 V).

We postulate then, that the type "A" and "B" Fe sites give rise to the overlapping voltammetric waves at 0.19 and 0.14 V and undergo electron self-exchange reactions at rates that differ by least 10-fold as revealed in Figure 5. It is certainly plausible that the more symmetrically substituted type "B" Fe should enjoy an elevated electron self-exchange rate.

At this point, it should be noted that the D_e data in Table I represent a composite of at least two electron-conduction pathways for KNO_3 electrolyte and, from analogous differences in $E^{\circ\prime}$ and $E_{1/2}$, probably for the other electrolytes as well. The (Table I) composite D_e in KNO_3 is, however, within a factor of 2 of the D_e value for the less conductive type "A" Fe (Figure 5), which is unsurprising since the predominant type "A" Fe contributes most of the charge, Q, in eq 1. Thus, our discussion above regarding the problem of *local* counterion mobilities applies strictly only to electron hopping between type "A" sites. It is less certain that *local* counterion mobility has no effect on the faster electron hopping between type "B" sites, but this seems likely given the persistent $E^{\circ\prime}$, vs. $E_{1/2}$ differences in Table I.

Steady-State Voltammetry. D_e for the Fe(III/II)–Fe(III/III) Mixed-Valent State in Contact with Aqueous KNO_3. The electron-hopping rate between the low-spin hexacyano sites in the Prussian blue film can be evaluated by scanning the potential of one Pt finger set on the IDA to 1.1 V (producing Fe(III/III) on that side of the film, Figure 6B) while maintaining that of the other at 0.5 V (producing Fe(III/II), Figure 6A). The limiting currents i_{lim} (at which point Fe(III/II) and Fe(III/III) gradients exist in the gap as in Figure 6C) are much larger[23,24] than those

(22) The D_e values obtained when Q_{sc} and i_{ss} both have significant values (Figure 5; between ca. 0.08 and 0.3 V) are clearly the most reliable results.

(23) The D_e measurement in Figure 6B was made on an IDA having a larger (ca. 10×) area than that used to obtain D_e in Figure 3B, partially accounting for the differing current scales. Nevertheless, the ratio of i_{lim} to Q is much increased; for this reason the current peaks visible in Figure 3B are not significant in Figure 6B.

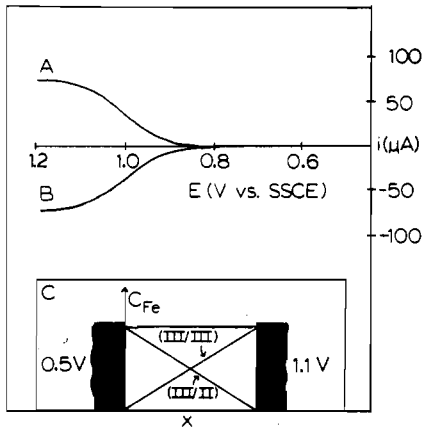

Figure 6. Steady-state oxidative voltammetry at a Prussian blue coated IDA immersed in 0.5 M KNO_3, pH 4: (B) current resulting when one terminal is scanned while the opposite terminal (A) is maintained at 0.5 V; (C) Fe concentration–distance profiles at potentials of plateaus in curves A and B. v = 5 mV/s. Prussian blue thickness is 0.75 μm.

in Figure 3 and with the charge Q for low-spin Fe in the IDA[25] yield an electron diffusion coefficient of 2.9×10^{-8} cm²/s. This value is similar to that observed above for the symmetrically substituted type "B" hexaisocyanoiron (Figure 5) and is a measure of the electron self-exchange rate constant between ferrocyanide and ferricyanide Fe sites in the Prussian blue lattice.

The electron diffusion coefficient D_e of the ferro–ferricyanide couple in Prussian blue is proportional to the apparent electron self-exchange rate constant, k_{ex}^{app}, according to the relation[26]

$$D_e = 10^3 k_{ex}^{app} C(\Delta X)^2 \quad (3)$$

where C is the concentration of the sites separated by an average distance ΔX. Taking ΔX = 7.25 Å from the "insoluble" structure[13] and $D_e = 2.9 \times 10^{-8}$ cm²/s, an apparent self-exchange rate constant of 1.3×10^6 M^{-1} s^{-1} results for the self-exchange rate constant between lattice ferricyanide and ferrocyanide sites. Electron self exchange rate constants reported[27] for ferrocyanide and ferricyanide dissolved in homogeneous solution are very sensitive to solution composition and range from 6 M^{-1} s^{-1} to 9.2×10^4 M^{-1} s^{-1}. The latter value, the largest solution rate constant we know of, is about 10 times slower than the value calculated above for the lattice ferro–ferricyanide reaction. There are several reasons eq 3 and an alternative calculation[8] based on the Smoluchowski equation[28] might *under*estimate the lattice self-exchange rate constant, but it is not obvious how it could ferricyanide a substantial *over*estimate. The cause(s) for this substantial lowering of the ferro–ferricyanide electron transfer barrier within the Prussian blue lattice are unclear, but could include a lattice-imposed structural similarity between the ferrocyanide and ferricyanide states.

Solid-State Voltammetry of Films Contacted Only by Gases. The third electron conductivity experiment conducted on Prussian blue involves simply exposing a coated IDA to a selected gas and slowly scanning a potential (ΔE) applied across the two terminals of the IDA. Current flows through the Fe(II/II) films when ΔE becomes large enough that simultaneous Fe(III/II) → Fe(II/II) reduction and Fe(III/II) → Fe(III/III) oxidation occur at opposing film/electrode interfaces; i.e., ΔE is large enough to disproportionate the Fe(III/II) Prussian blue. Further, if the ΔE potential scan is slow enough that steady-state concentration gradients of Fe(III/III), Fe(III/II), and Fe(II/II) and associated counterions can be established and maintained, then the current flowing through the film will vary with ΔE in a voltammetric wave shape.

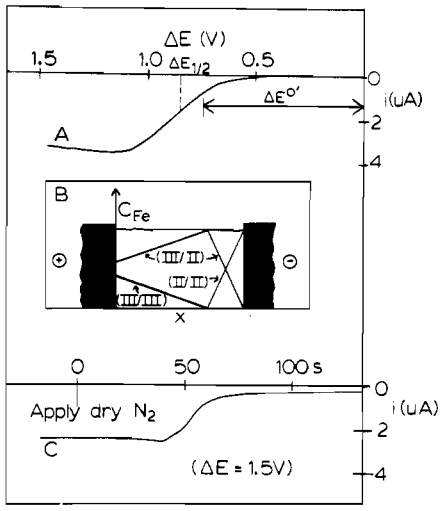

Figure 7. Solid-state voltammetry at a Prussian blue coated IDA: (A) two-electrode voltammetry in air, v = 20 mV/s; (B) approximate Fe concentration distance profiles at ΔE = 1.5 V; (C) current–time transient showing effect of water removal at ΔE = 1.5 V.

Figure 7A shows such a *solid-state voltammogram*, which indeed has $E_{1/2}$ = 0.85 V, which matches approximately the difference $\Delta E^{0'}$ between the formal potentials for Fe(III/II) → Fe(II/II) reduction and Fe(III/II) → Fe(III/III) oxidation, 0.75 V. We should emphasize the novelty of this experiment, showing that electrochemical voltammetry is possible in the absence of a bathing solvent, and distinguish it from other solid-state electrochemical reactions[29] in which electrochemical charging is accomplished but without achieving the kind of steady-state concentration gradients across the sample that Figure 7B represents.[30] The key aspect of the present experiment is that the path lengths over which electrons and ions must move to achieve the steady state and thus the time to achieve the steady state are short.

Three significant observations were made from the solid-state experiments. First, voltammograms like Figure 7A and their limiting currents were *very stable* when observed with the coated IDA simply exposed to laboratory room air. This made it convenient to conduct in situ optical microscopy on the coated IDA in which the two Pt finger pairs could be observed, as ΔE was scanned, to change color from a uniform blue to green and white and then, at 1.5 V, on the plateau of the Figure 7A voltammogram, to golden and white. These are the reported colors of Fe(III/III)[3a] and Fe(II/II). (The capability for in situ microscopic observations on a functioning electrochemical cell is an important attribute of the open IDA geometry and, given the proper system, should be generalizable to more powerful techniques, such as UPS and energy-dispersive X-ray (EDX) spectroscopy.) The color ob-

(24) It has been suggested,[2b] on the basis of cyclic voltammetric peak currents, that the rate of oxidation of Prussian blue is slower than its reduction. Our D_e results show that electron transport is, instead, faster for the oxidation. The large ΔE_p observed[2b] in the oxidation voltammetry (which we confirm[14]) is probably associated with slow ion (rather than electron) transport during *net* change of the counterion population in the film.

(25) Ideally, D_e should be evaluated by using Q_{ox} obtained from oxidative cyclic voltammetry. Due to the instability of the Fe(III/III) state, this was not done. Q_{ox} was calculated to equal 0.75 Q_r, from the stoichiometric formula $Fe_4(Fe(CN)_6)_3$.

(26) Andrieux, C. P.; Saveant, J.-M. *J. Electroanal. Chem. Interfacial Electrochem.* **1980**, *111*, 377.

(27) (a) Campion, R. J.; Deck, C. F.; King, P.; Wahl, A. C. *Inorg. Chem.* **1967**, *6*, 672. (b) Shporer, M.; Ron, G.; Loewenstein, A.; Navon, G. *Inorg. Chem.* **1965**, *4*, 361.

(28) On the basis of arguments we have presented,[8] k_{ex}^{app} can alternatively be calculated by using the Smoluchowski equation, $k_{ex}^{app} = (4 \times 10^{-3})\Delta X D_e N$, which gives a value ($1.6 \times 10^7$ M^{-1} s^{-1}) about 10 times larger than that from eq 3.

(29) (a) Raleigh, D. O. In *Electroanalytical Chemistry*; Bard, A. J., Ed.; Marcel Dekker: New York, 1973; Vol. 6, (b) Skotheim, T. A.; Florit, M. I.; Melo, A.; O'Grady, W. E. *Mol. Cryst. Liq. Cryst.* **1985**, *121*, 291. (c) Skotheim, T.; Florit, M. I.; Melo, A.; O'Grady, W. E. *Physical Review B* **1984**, *30*, 4846.

(30) Analogous two-electrode experiments, albeit in solvent/electrolyte, have also been reported[11e] for microarray electrodes coated with spatially discrete films of poly(vinylferrocene) and an *N,N'*-dibenzyl-4,4'-bipyridinium-based polymer.

servations support our assertion that the stable[31] solid-state voltammogram of Figure 7A corresponds to the production of Fe(III/III) at one Pt finger and Fe(II/II) at the opposite finger, with subsequent conproportionation to Fe(III/II) in the intervening gap as illustrated in Figure 7B.

The second observation relates to the question of maintaining electroneutrality at all points within the film during solid-state voltammetry. We have pointed out in analogous experiments[32] with (sandwiched) films of $([Os(bpy)_2(vpy)_2](ClO_4)_2)_n$ that electroneutrality of the film in the absence of an external supporting electrolyte solution requires an internal supply (which we called the ion budget) of resident, mobile counterions. Thus, in order to generate the gradients of Fe(III/III), Fe(III/II), and Fe(II/II) sites illustrated in Figure 7B (which are drawn asymmetrically in view of the larger D_e values for the Fe(III/III)/Fe(III/II) couple), some ionic species in the Prussian blue film must migrate from one side of the film to the other. Pretreatment of an as-grown Prussian blue film by cycling through the Fe(III/II) → Fe(II/II) reduction in aqueous KNO_3 enhances the solid-state currents that can be observed by ca. 10 times. We associate this effect with the incorporation of K^+ into the film that accompanies electrochemical cycling and a consequently larger ion budget that allows more complete charging of the film.

The third observation relates to the effect of water vapor on the solid-state currents. In experiments conducted in laboratory air, we saw that the solid-state limiting currents appeared to vary directly with the local humidity around the cell. In fact, observation of current through the film was critically dependent on the presence of water vapor in the IDAs bathing environment. If no water vapor, but only dry N_2, is present in the bathing gas, scanning the potential difference ΔE between the IDA finger sets produces no detectable current. More strikingly, if an IDA that has already been polarized at $\Delta E = 1.5$ V in moist air, is placed in a dry N_2 atmosphere, after a short period the current decays to a small value (Figure 7C), yet the IDA fingers *remain* white and golden. The colors persist even when ΔE is returned to zero in an attempt to discharge the IDA. The concentration gradients of Figure 7B are, remarkably, frozen in place by the drying of the Prussian blue film. Thus, the presence of water molecules, probably occupying interstitial sites, is necessary for electron conduction, even in morphologically intact Prussian blue films. This result is analogous to that reported recently[21] on the importance of solvent molecules for intramolecular electron transfer in mixed-valent, oxo-centered, trinuclear iron acetate complexes.

We propose that the importance of the interstitial water is that it acts to solvate internal counterionic species in the Prussian blue film and thereby exerts control over their mobility. Desolvation of the charge-compensating counterions would elevate the barrier associated with local displacements of the counterion accompanying electron hopping that was illustrated above. The results thus form a most interesting contrast. In water-wetted Prussian blue, we deduced from the results in Table I that the local ionic mobility is sufficiently high that D_e for the Fe(III/II) → Fe(II/II) couple is not sensitive to the choice of local cation (among K^+, NH_4^+, Rb^+, and Cs^+). In the absence of water in the solid-state experiment, on the other hand, the local ionic mobility can be made so slow as to control, and close off, the electron-hopping process.

Acknowledgment. This research was supported in part by grants from the National Science Foundation and the Office of Naval Research. Helpful discussions with C. Lundgren (UNC) and SEM micrography by R. Kunz (UNC) are gratefully acknowledged.

Registry No. $Fe_4[Fe(CN)_6]_3$, 14038-43-8; $KFe[Fe(CN)_6]$, 25869-98-1; $NaNO_3$, 7631-99-4; KNO_3, 7757-79-1; NH_4Cl, 12125-02-9; RbCl, 7791-11-9; $RbNO_3$, 13126-12-0; CsCl, 7647-17-8; H_2O vapor, 7732-18-5.

(31) The electrochemistry of the Fe(III/III) state is highly stabilized in moist air relative to films exposed to aqueous electrolytes ($t_{1/2}$ for decay during cyclic voltammetry is ca. 1 min. in KNO_3). Consequently, it proved possible, by the use of a square wave ΔE, to cycle the film between the blue ("off", Fe(III/II)) form and the golden/white form in ambient air a total of 2×10^4 times over 3 days with little change in current (500-ms transient) or color response. The removal of decay–reaction pathways associated with solvents and trace impurities therein may be an unforeseen but general attribute of solid-state voltammetry.

(32) Jernigan, J. C.; Chidsey, C. E. D.; Murray, R. W. *J. Am. Chem. Soc.* **1985**, *107*, 2824.

(33) Some cracking of the film does probably occur upon drying, but this cannot account solely for the above result, since if the film is reexposed to water vapor, currents are again observed, albeit at lower values.

Contribution from the Chemistry Department, Royal Veterinary and Agricultural University, DK-1871 Frederiksberg C, Denmark, and Department of Chemistry, University of California at San Diego, La Jolla, California 92093

Aqueous Solution Photophysics and Photochemistry of Dihalo- and Aquahalobis(ethylenediamine)rhodium(III). Effect of Nonreacting Amine Ligands on Excited-State Halide Dissociation and Excited-State Rearrangement

L. H. Skibsted,*[1] M. P. Hancock,[1] D. Magde,*[2] and D. A. Sexton[2]

Received March 25, 1986

Ligand field excitation of *cis*- and *trans*-$[Rh(en)_2X_2]^+$ (X = Cl, Br) in acidic aqueous solution leads to halide photoaquation producing $[Rh(en)_2(H_2O)X]^{2+}$. Room-temperature phosphorescence lifetimes of the four dihalo complexes in aqueous solution were measured by using a mode-locked laser and time-correlated single-photon detection and found to be about 2 ns in each case. Excited-state halide dissociation and nonradiative deactivation rate constants were evaluated from a combination of the lifetimes and the photoaquation quantum yields. The halide dissociation rate constants range from 1.9×10^8 (*cis*-dichloro) to 2.1×10^7 s^{-1} (*trans*-dibromo) and are in all cases smaller (by a factor of 1.6–15) than the rate constants previously determined for the tetraammine and bis(1,3-propanediamine) analogues. Also described are the syntheses of the dithionate salts of *trans*- and *cis*-$[Rh(en)_2(H_2O)X]^{2+}$, and quantum yields for the cis/trans interconversion of each isomeric pair in aqueous solution at 25 °C are given.

Introduction

Haloaminerhodium(III) complexes undergo efficient and highly stereomobile photosubstitution reactions when irradiated with light of energy matching the multiplicity allowed ligand field transitions. This photoreactivity has been traced to thermally equilibrated lowest energy triplet ligand field states populated by efficient internal conversion and intersystem crossing from the initially populated singlet ligand field states.[3-5] Haloaminerhodium(III) complexes show weak dual photoluminescence, and the longer-lived

(1) Royal Veterinary and Agricultural University.
(2) University of California at San Diego.

(3) Ford, P. C. *Coord. Chem. Rev.* **1982**, *44*, 61.
(4) Ford, P. C.; Wink, D.; DiBenedetto, J. *Prog. Inorg. Chem.* **1983**, *30*, 213.
(5) Skibsted, L. H. *Coord. Chem. Rev.* **1985**, *64*, 343.

0020-1669/87/1326-1708$01.50/0